Simple qualitative description of EMC ratios for $0.2 \lesssim x \lesssim 1.4$ and some sample calculations

A.S.Rinat

I. INTRODUCTION.

We start with a synopsis: Two generations of 'direct' experiments.

a) First some 20 yrs ago, low Q^2.

b) Second at much higher Q^2, down to very low x: revisions of previous ones. Canon closed some 10 years ago.

Indirect information: Use independent data sets on F_2^A and F_2^D with similar kinematics. Many years ago, EMC ratios extracted for relatively low Q^2 (SLAC NE3) data out to $x \approx 1.5$. Below exploitation of JLab E89-008 data at much higher Q^2. Additional info: Drell-Yan.

Observations:

i) In classical regime $0.2 \lesssim x \lesssim 0.9$, $|1 - \mu^A(x, Q^2)|$ between ≈ 0 and 0.15-0.20; little A, Q^2 dependence.

ii) In adjacent range $0.95 \lesssim x \lesssim 1.05$, sharp rise in extracted EMC ratios for $Q^2 \lesssim (3.5 - 4.0)$ GeV^2, immediately followed by an abrupt decrease: minima around $x \approx 1$; depth depends on A, Q^2.

iii) 'Deep'-QE region $1.05 \lesssim x \lesssim 1.5$, EMC ratios resume rise. Slope increases with Q^2. μ^A reach maxima of order 4-7, which level off. Very small, increasingly imprecise composing $F_2^{A,D} \rightarrow$ scatter in present-day μ^A.

Most explanations concentrate on classical range; use (PWIA). Different versions: no unanimously accepted understanding. Do Fermi averaging + binding corrections explain or not? Frustration led to occasionally far-flung approachesas are use of Bethe-Salpeter equations for vertex functions, medium modifications of nucleons the introduction of, in the EMC field exotic chiral solitons, etc.

Two reasons to-reopen nearly stalled discussion:

a) Running JLab E03-103 inclusive scattering exp. on D, ^{3}He and ^{4}He. Modern He data were missing; will now extend beyond $x = 1$.

b) Is it possible to give a simple understanding of EMC ratios?

Beware of pitfalls in over-simplification: Example: why do ratios μ^A for $x \gtrsim 0.9$ rise

towards $x = 1$? Off-hand one expects $F_2^D(x \lesssim 1)$ to become very small, because SFs of free p, n vanish for $x \to 1$. Can weak binding make much difference? If not, $\to F_2^D$ small for $x \to 1$. However, similar decrease for all heavier targets, and actually more so. Result: μ^A may have deep *minima* for $x = 1$. For growing x SFs continue to decrease: Can one trust computations?

In spite of the above skepsis, attempt of such a description.

II. GENERALITIES.

Postulated relation between SF $F_k^{N,A}$ for nucleons ($N = p, n$) and a nucleus

$$F_2^A(x, Q^2) = \int_x^A dz f^{PN,A}(z, Q^2) F_2^{\langle N \rangle}\left(\frac{x}{z}, Q^2\right) \tag{2.1a}$$

$$= \int_{1/A}^{1/x} du B^A(u, Q^2) F_2^{\langle N \rangle}(xu, Q^2), \tag{2.1b}$$

with

$$B^A(u, Q^2) = f^{PN,A}(1/u, Q^2)/u^2 \tag{2.2}$$

and

$$F_2^{\langle N \rangle} = \frac{F_2^p + F_2^n}{2} + \frac{\delta N}{2A}(F_2^p - F_2^n), \tag{2.3}$$

Integrands separate x and A dependence.

Connection between nuclear and averaged nucleon SF,described by $f^{PN,A}$. It is the SF of a fictitious target A, composed of point-nucleons. Above Eqs. describe partons, which originate from nucleons: Disregard $x \gtrsim 0.2$.

Interlude: Separate $F^N = F^{N,NE} + F^{N,NI}$ for absorption of the exchanged virtual photon by a N, respectively exciting N. In particular $F_2^{N,NE} = \delta(1-x)\mathcal{G}_2(Q^2)$, with $\mathcal{G}_2(Q^2)$, linear combination of nucleon form factors. Substution in link equation:

$$F_2^{A,NE}(x, Q^2) = f^{PN,A}(x, Q^2)\mathcal{G}_2(Q^2) \tag{2.4}$$

SF f depend on many-body target density matrices, diagonal in all except one coordinate. Can be calculated with precision for $A \leq 4$. Also required: info on (off-shell) NN scattering.

Salient properties of $f^{PN,A}$:

a) $f^{PN,A}(x, Q^2)$ are normalized, smooth functions of x. Have Q^2-dependent maximum $x_M(Q^2) \lesssim 1$ close to QE peak (Fig.1).

b) For given Q^2, peak-values decrease with A from D, He $\rightarrow$ general A. Only few % differences between nuclei with $A > 12$. Due to normalization $\rightarrow$ widths of f show marked variations with $A < 12$ (Fig. 1).

c) Peak-values of all f increase with Q^2 (Figs. 2).

d) Ratios of peak values $f^{PN,A}$ for $x \approx 1$ only weakly Q^2 dependent.

Disregarding small δN effects, from Eqs. (2.1): A-dependence of nuclear SFs is governed by same in $f^{PN,A}$.

Properties of B^A, Eq. (2.1b) from those of $f^{PN,A}$. Figs. 3 for a few targets and for $Q^2 = 3.5, 10\,\mathrm{GeV}^2$. B^A peaks around $u \approx 1$ and decreases on both sides with increasing $|1-u|$, and due to $1/u^2$ in a more asymmetric fashion than $f^{PN.A}$. Like f, B^A ordered as function of A. For $A \gtrsim 12$ B^{D} at $u_i \approx 0.9$. B^{D} and $B^{^4\mathrm{He}}$ cross at $u_i < u_i^A$.

$$B^{\mathrm{D}} > B^{^4\mathrm{He}} > B^{\mathrm{Fe}} \approx B^{\mathrm{C}} > B^{\mathrm{Au}} \quad ; 1.1 \gtrsim u \gtrsim 1.0, \tag{2.5a}$$

$$B^{\mathrm{D}} \ll B^{\mathrm{Fe}} \approx B^{^4\mathrm{He}} \lesssim B^{\mathrm{C}} \approx B^{\mathrm{Au}} \quad ; u \lesssim 0.9 \tag{2.5b}$$

III. CHARACTERISTIC FEATURES OF EMC RATIOS.

Unless stated otherwise, we consider the usually dominant NI parts of both SF in EMC ratios.

A. The classical range $0.2 \lesssim x \lesssim 0.90$.

I) Observation: slope of $F_2^{p,D}(x,Q^2)$ as function of Q^2 vanishes for $x_1 \approx 0.18 - 0.20$. Small enough for validity of

$$F_2^n(x,Q^2) \approx 2F_2^D(x,Q^2) - F_2^p(x,Q^2) \tag{3.1}$$

Same for $F_2^{\langle N\rangle}$, Eq. (2.3) in (2.1). Use property a) in Eq. (2.1a), For $x' \approx 0.18 \ll x \approx 1$ and independent of A,

$$F_2^A(x',Q^2) = \int_{x'}^{A} dz f^{PN,A}(z,Q^2) F_2^{\langle N\rangle}\Big(\frac{x'}{z},Q^2\Big)$$

$$\approx F_2^{\langle N\rangle}(x',Q^2) \quad \int_0^A dz f^{PN,A}(z,Q^2) = F_2^{\langle N\rangle}(x',Q^2) \tag{3.2a}$$

$$\frac{\partial F_2^A(x)}{\partial x}\Big|_{x=x'} \approx \frac{\partial F_2^{\langle N\rangle}(x)}{\partial x}\Big|_{x=x'} \tag{3.2b}$$

For lowest x, independent of A and Q^2, $\mu^A(x_1 \approx (0.18 - 0.20, Q^2) \approx 1$. Observed for all data.

Need also shape of $F^{\langle N\rangle}$: decreases with increasing argument; ≈ 0 for $xu \gtrsim 0.80$

II) Consider B^A * weighted nucleon SF $F_2^{\langle N\rangle}(xu,Q^2)$

For small x, argument xu of F^N can be $\lesssim 0.6 - 0.7$ for most u, including the peakvalue $u = 1$ of B^A. For increasing x less and less small xu contribute $\rightarrow$: integrand decreases. Fig. 4 for He, Fe and Au. From $x = 0.1 \rightarrow 0.5 \rightarrow 0.85 \rightarrow 1.2$ integrand drops by ≈ 10. Resulting ordering $F_2^{\rm D} > F_2^{^4{\rm He}} > F_2^A$ and thus for EMC ratios

$$\mu^A < \mu^{^4{\rm He}} < 1 \; ; 0.2 \lesssim x \lesssim 0.75 \tag{3.3a}$$

$$\mu^{^4{\rm He}} \approx \mu^A > 1 \; ; 0.75 \lesssim x \lesssim 0.90 \tag{3.3b}$$

III) Factors in integrand are smooth $\rightarrow$ a second intersection point at $x_2^A \approx 0.85$. From A-dependence of u_i^A, $(B^D(u_i^A) = B^A(u_i^A))$ x_2^A larger for ^{4}He (and even more for ^{3}He) than for $A \gtrsim 12$.

IV) Slopes $s^A(x,Q^2) = \partial\mu^A(x,Q^2)/\partial x$ at $x_{1,2}$. From Eqs. (3.2): all SFs and their slopes are about equal for $x \approx 0.2$: small, nearly A-independent slope ≈ -0.3 around x_1. Slope around $x \approx x_1$, $s^A(x \approx x_2^A)$ is positive and large. Agrees with observation .

For constant slopes minimum $x_m \approx 0.6 \gtrsim (x_1 + x_2^A)/2 \approx 0.65$. Actual value $\mu^A(x = x_m, Q^2)$ requires x-dependence of $s^A(x)$.

B. The immediate QE peak region $|x-1| \lesssim 0.05$.

V) Further increasing x towards QE region $x \approx 1$. Non-negligible $F_2^N(ux)$ for $x \gtrsim 0.9$ requires $u \ll 0.8$ in elastic tails of $B^A(u) \to B^A > B^D$ and

$$\mu^A < \mu^{^4\mathrm{He}} < 1 \quad ; 1.05 \gtrsim x \gtrsim 0.95 \tag{3.4}$$

NI components dominate, except around the QE region for $Q^2 \lesssim 2.5\,\mathrm{GeV}^2$ and light targets.

Relative weights $\gamma^A = F_2^{A,NI}/F_2^{A,NE}$ in total $F_2^A = F_2^{A,NI} + F_2^{A,NE}$. Auxiliary EMC ratios $\mu^{A,NI}, \mu^{A,NE}$

$$\mu^A = \mu^{A,NI}\frac{\left[1+(\gamma^A)^{-1}\right]}{\left[1+(\gamma^D)^{-1}\right]} \tag{3.5a}$$

$$\approx \mu^{A,NI} \qquad ; Q^2 \gtrsim 4\mathrm{GeV}^2; x \lesssim 0.95,\ x \gtrsim 1.05 \tag{3.5b}$$

$$\approx \mu^{A,NE}\frac{\left[1+\gamma^A\right]}{\left[1+\gamma^D\right]} \qquad ; A \leq 4; Q^2 \lesssim (2.5-3.0)\,\mathrm{GeV}^2; |x-1| \lesssim 0.05 \tag{3.5c}$$

Eq. (3.5b): when dominant, NI components hardly perturbed by NE. For $A \leq 4$ and $Q^2 \lesssim (2.5-3.0)\,\mathrm{GeV}^2$ reversed situation, with $\gamma^A \ll 1$. In (3.5c), non-negligible competition of NI components, even where NE is maximal. Without NI

$$\mu^A(x \approx 1, Q^2) \approx \mu^{A,NE}(x \approx 1, Q^2) = \frac{f^{PN,A}(x \approx 1, Q^2)}{f^{PN,D}(x \approx 1, Q^2)} \ll 1, \tag{3.6}$$

Like $f^{PN,A}$ roughly symmetric around $x \approx 1$. Sharp increase of μ^A beyond value 1 for $x_2 \approx 0.85-0.90$. Then equally abrupt decrease into local minimum. Relative A-dependence: from Fig. 1.

$$\mu^{\mathrm{C}}(x \approx 1) \approx \mu^{\mathrm{Fe}}(x \approx 1) < \mu^{\mathrm{He}}(x \approx 1) \lesssim 1 \tag{3.7}$$

For low Q^2, the depth of the minimum is ≈ 0.35 for $A \geq 12$, and only ≈ 0.50, respectively ≈ 0.50 for $A = 4, 3$. For medium Q^2 $NI < NE$ and position of the minimum at $x \approx 1$ hardly dependent on Q^2. For increasing Q^2, NI rapidly grows relative to NE $\rightarrow$ specific NE effect submerged in NI. Minima at $x \approx 1$ gradually vanish and μ^A, more or less continuously grows from $x \approx 0.85$.

C. The 'deep' QE region.

VI) For further increasing x, above shows diminmishing B^A and argument xu makes F_2^N and thus nuclear SF F_2^A very small (cf. Fig. 4). What about ratios of two SF?

Figs. 3 show that for sufficiently small u all B^A decrease with a characteristic A-dependence. For fixed u, D fast decrease is prominent. Decrease is less for He, Fe and A. Figs. 3 also show Q^2-dependence $\rightarrow$: EMC ratios increase for $x \geq 1.05$ to values $\ll 1$ in A, Q-dependent fashion.

End of more than heuristic description. Understanding orderings does not require precise values of small values of nuclear SF: derives from qualitative features of $B^A(u, Q^2), f^{PN,A}(x, Q^2)$ and simple functional behavior of $F_2^{\langle N \rangle}(xu)$.

Remark on generalized EMC ratios. Until thisa point: EMC ratios of F_2^A and F_2^D. Same considerations for ratios of F_2^A with $F_2^{\langle N \rangle}$ (weighted SF of nucleon).

Quantitavely different for generalized EMC ratios $\mu^{A,A'}$, $A' \geq 12$: above predicts deviations of $\mu^{A,A'}$ from 1 by no more than a few %. NB: He isotopes are special: In classical regime $\mu^{A,^4\mathrm{He}} < \mu^{A,^3\mathrm{He}} < \mu^{A,D}$: Egyan data on EMC ratios $\mu^{A,^3\mathrm{He}}$ show all features of μ, but in a more temperate fashion.

IV. INPUT, RESULTS.

Quntification of above needed. Be aware, that values of $F_2^{A,D}$ rapidly decrease with increasing x. One must be ambitious or over-confident to expect close agreement with data.

a) SF $f^{PN,A}$ for nuclei, composed of point-nucleons: accurate calculations for lightest nuclei. For $A \geq 4$ unavoidable approximations.

b) Applications for $Q^2 \geq 3.5$ GeV^2. Use parametrization of resonance-averaged F_2^p instead of data on F_2^p itself.

c) F_k^n not-directly accessible. Used model for extraction from inclusive scattering data.

Question: what F_2^D in the denominator of μ^A? Off-hand seems best to use experimental values. We advocate the computed F_2^D; has same 'systematic' theoretical insufficiencies for all F_2^A: may cancel in ratios. Minor practical relevance: computed F_2^D agree well with resonance-averaged parametrizations.

Figs. 5,6,7,8 for ^{4}He, C, Fe and Au.: Data and computed EMC ratios for $Q^2 = 3.5, 5.0, 10.0\,\mathrm{GeV}^2$ over two separated ranges $0.2 \lesssim x \lesssim 0.95$ and $x \geq 0.95$.

In classical range: original data, revised ones and newer data (closed circles). Occasionally averages as compiled by Gomez. Results confirm insensitivity to Q^2, except for $Q^2 = 3.5\,\mathrm{GeV}^2$: Some structure caused by irregular F_2^A for $x = 0.7$.

In DI region reasonable, not perfect agreement. QE peak at $x = 1$: noticible inelastic NI effects over and above NE ratios $\mu^{A,NE}$, Eq. (3.7).

Empty squares: extracted data only for $Q^2 = (3.4 - 4.2)$ GeV^2 . Filed squesres for $Q^2 = (4.5 - 5.3)$ GeV^2. Theoretical curves are for $Q^2 = 3.5, 5.0\,\mathrm{GeV}^2$: no interpolations in data for mildly varying Q^2.

Given the sensitivity and small numbers, agreement in deep QE region also satisfactory. Results in line with all qualitative predictions.

Presently running Jlab EMC experiment E03-103 will provide a test for the Q^2-dependence for He isotopes for wide x-range, crossing $x = 1$. Will no doubt show vanishing of minimum.

V. DISCUSSION, COMPARISON AND CONCLUSION.

All along aware, that composing nuclear SF in EMC ratios decrease two orders of magnitude from ≈ 0.37 for very small x, up to $x \approx 1$: there up to $10-20\%$ deviations of EMC ratios from 1. Required $\rightarrow$ computations, more accurate than the size of the EMC effect! Requirement seems impossible for x increasing x to 1.4-1.5: involved SF decrease by another two orders.

Tool of analysis: postulated relation between nuclear and nucleon SFs, linked by $f^{PN,A}$, the SF of an unphysical nucleus, composed of point-particles.

Characteristics of f as function of x, Q^2 and A and on the x, Q^2-dependence of the properly weighted nucleon SF $F_2^{\langle N \rangle}$, allow simple qualitative account of *all* characteristic features of EMC ratios in the classical regime $0.2 \lesssim x \lesssim 0.95$, the QE peak area $0.95 \lesssim x \lesssim 1.05$, and continuing into the 'deep QE region' $1.05 \lesssim x \lesssim 1.5$, including the A dependence of μ^A. The same considerations carry over to the generalized ratios $\mu^{A,\mathrm{He}}$, in particular for ^{3}He, and data for the latter confirm those.

Qualitative considerations quite reliable: Mostly ordering or inequalities of quantities. Actual calculations of EMC ratios should be less reliable!

Results: reasonable agreement with data in classical range ($0.2 \lesssim x \lesssim 0.9$) and with extracted information for $0.9 \lesssim x \lesssim 1.5$.

Emphasis on simplicity and trasparancy, solely based on properties of SFs $f^{PN,A}$ and F_2^N. No a judgement against other approaches, e.g. DWIA. Liuti and Benhar et al. reach much the same results as above in deep QE region.

Different insights in some aspects of EMC ratios: minima in $\mu^A(x \approx 1)$. No particular role in the DWIA for QE point. Similarly Frankfurt and Strikman: allocate minimum to ratio of the longitudinal momentum distributions. In DWIA, one has to neglect FSI and to concentrate the spectral function in one peak. Not obviously equivalent to dominance NE in GRS approach.

F.S. explanation of plateau regions for $x \lesssim 1.5$: struck nucleon participates in ever higher,

diagonal multi-nucleon correlations. GRS theory for $x \lesssim 1.5$, incorporates not-completely diagonal multi-nucleon density matrices to first and second order.

Conclusion: GRS theory rather simply explains all features of EMC ratios, and their A, Q^2 dependence by properties of $f^{PN,A}$ anf F_2^N. No understanding why ratios of ever smaller nuclear SF appear to agree with data out to large x. Understanding remains a challenge.

VI. ACKNOWLEDGMENT.

Co-workers: M.F. Taragin and M. Viviani; John Arrington for providing much information and critical remarks.

TABLES

TABLE I. Target ordering of $B^A(u, Q^2)$, Eq. (2.4), as function of u, Q^2. The same for nuclear SF $F_2^A(x, Q^2)$ and EMC ratios $\mu^A(x, Q^2)$ as function of x, Q^2 (Q^2 is in units GeV^2). When not distinguishing between C, Fe, Au, we use A for all.

Function ordered targets	u, x interval	u, x interval	u, x interval	u, x interval
	$0.6 \leq u \leq 0.9$	$0.95 \leq u \leq 1.05$	$1.05 \leq u \leq 1.1$	$u \geq 1.1$
$B^A(u, Q^2 \leq 10)$	He $\gtrsim$ A $\gg$ D	D $\gg$ He $>$ A	He $>$A$\gg$ D	A$>$ He $\gg$ D
	$0.4 \leq x \leq 0.8$	$0.85 \leq x \leq 0.95$	$0.95 \lesssim x \lesssim 1.05$	$1.1 \lesssim x \lesssim 1.5$
$F_2^A(x, 3.5, 5.0)$	D $>$ He $>$ C $\gtrsim$ Fe	D $\gtrsim$ A	C $>$ He $\approx$ Fe $\gg$ D	C $>$ Fe, He $\gg$ D
$F_2^A(x, 10.0)$	D $>$ He $>$ C $\gtrsim$ Fe	C $>$ He $>$ Fe $\gg$D	C $>$ He $>$ Fe $\gg$ D	C $\gg$ He, Fe$\gg$D
	$0.3 \lesssim x \lesssim 0.75$	$0.9 \lesssim x \lesssim 1.05$	$x = 1.15$	$x = 1.3$
$\mu^A(x, 3.5)$	He $>$ C $>$ Fe	C $>$ He $>$ A	C $>$ Fe$\gtrsim$He$>$Au	C $\gg$Fe$>$He$>$Au
$\mu^A(x, 5.0)$	He $>$ C $>$ Fe	C $>$ He $>$ A	C $\gg$ Fe$>$He	C $\gg$Fe$>$He$>$Au
$\mu^A(x, 10.0)$	He $>$ C $>$ Fe	C $>$ He $>$ A	C $\gg$He$>$Fe	C $\gg$He$\gtrsim$Fe$>$Au

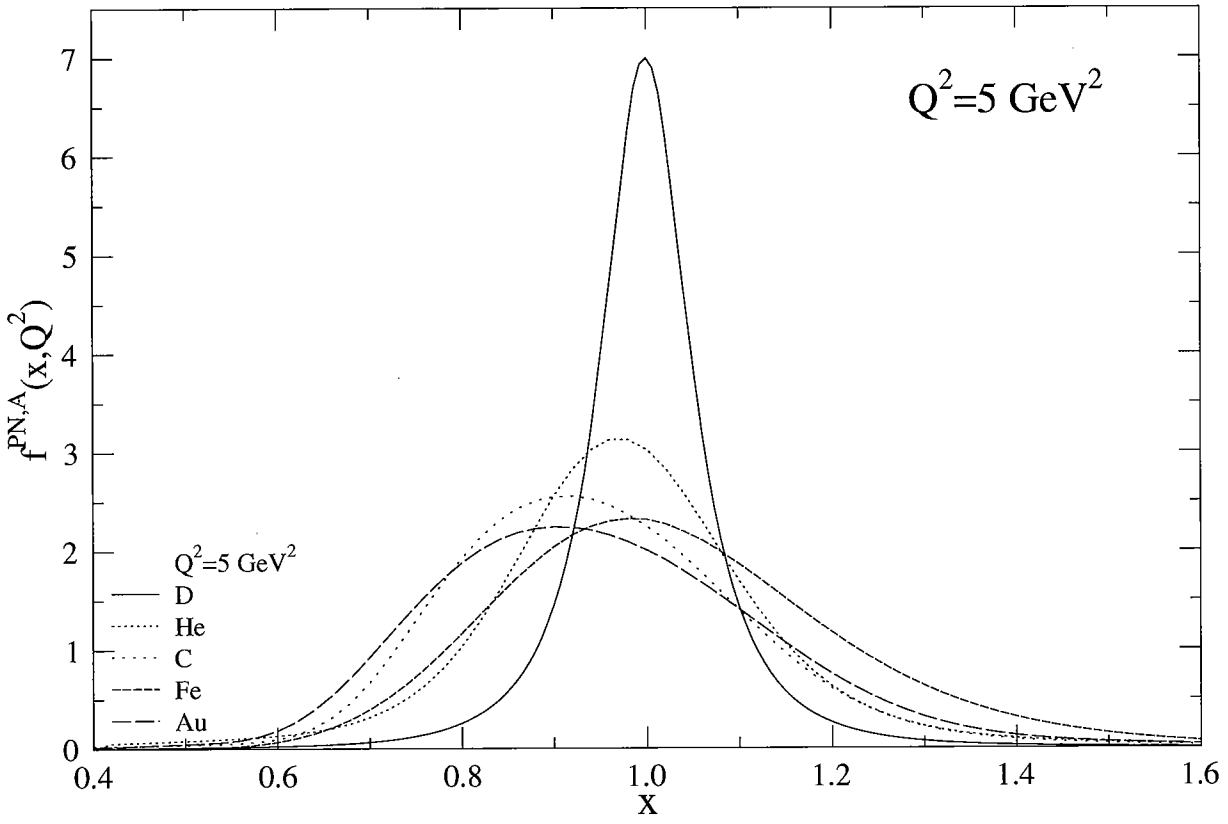

FIG. 1: The point-nucleon nuclear SF $f^{PN,A}(x,Q^2)$ for D, ^{4}He, Fe, C and Au; $Q^2 = 5\,\mathrm{GeV}^2$.

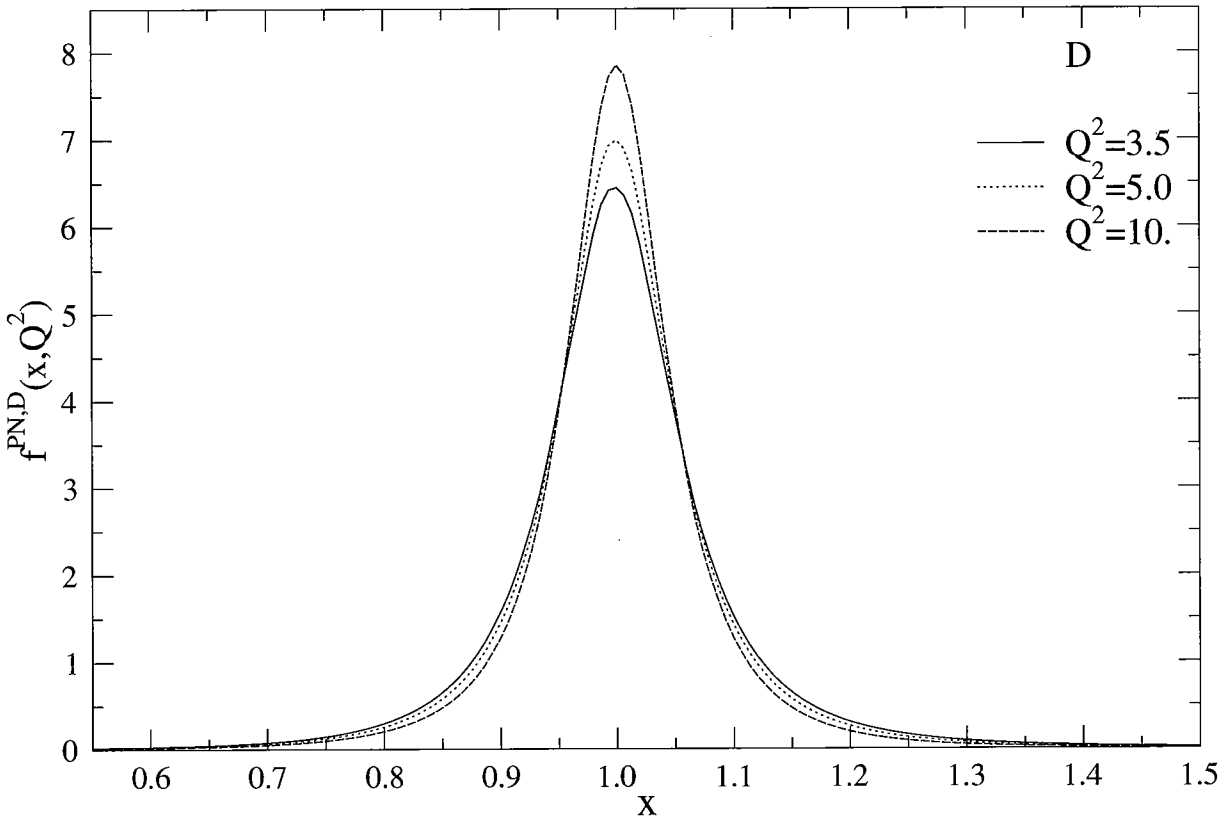

FIG. 2: Same as Fig. 1 for D at $Q^2 = 3.5, 5, 10\,\mathrm{GeV}^2$.

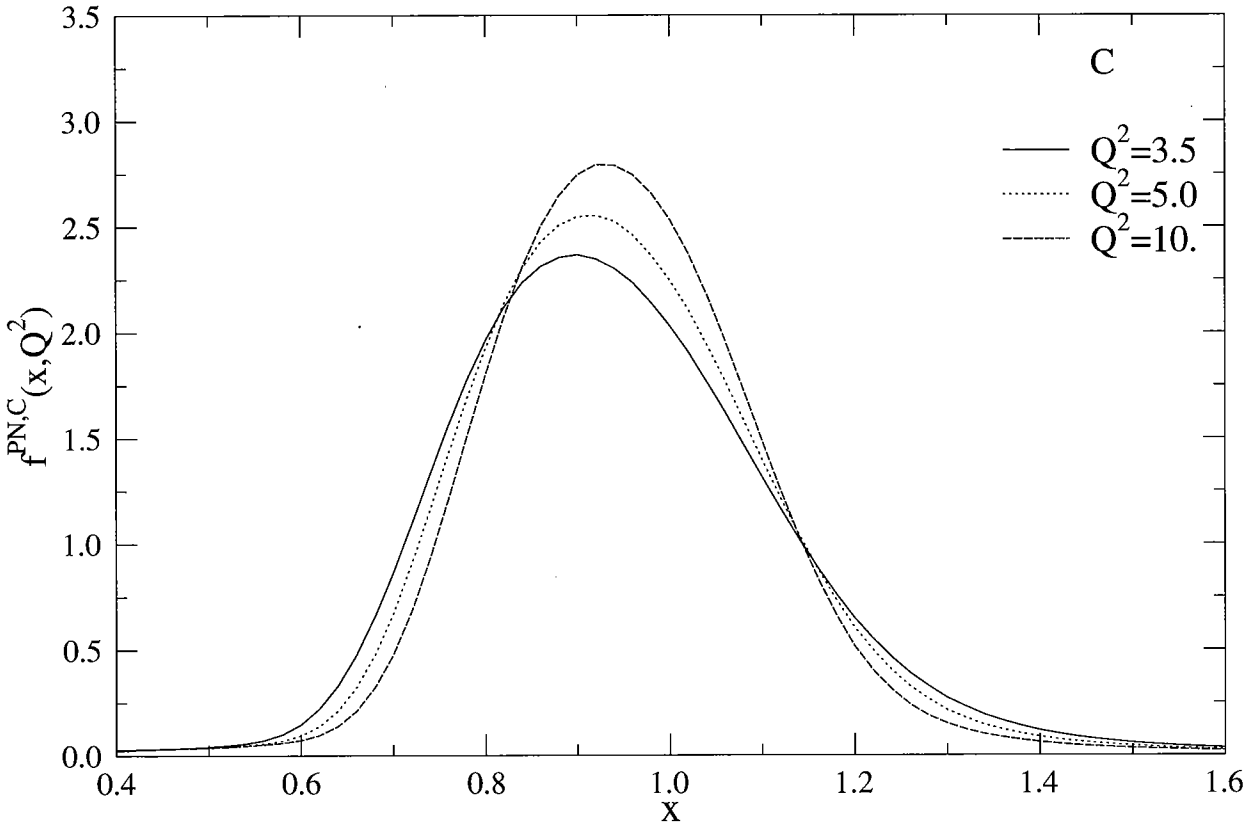

FIG. 3: Same as Fig. 1 for C at $Q^2 = 3.5, 5, 10\,\mathrm{GeV}^2$.

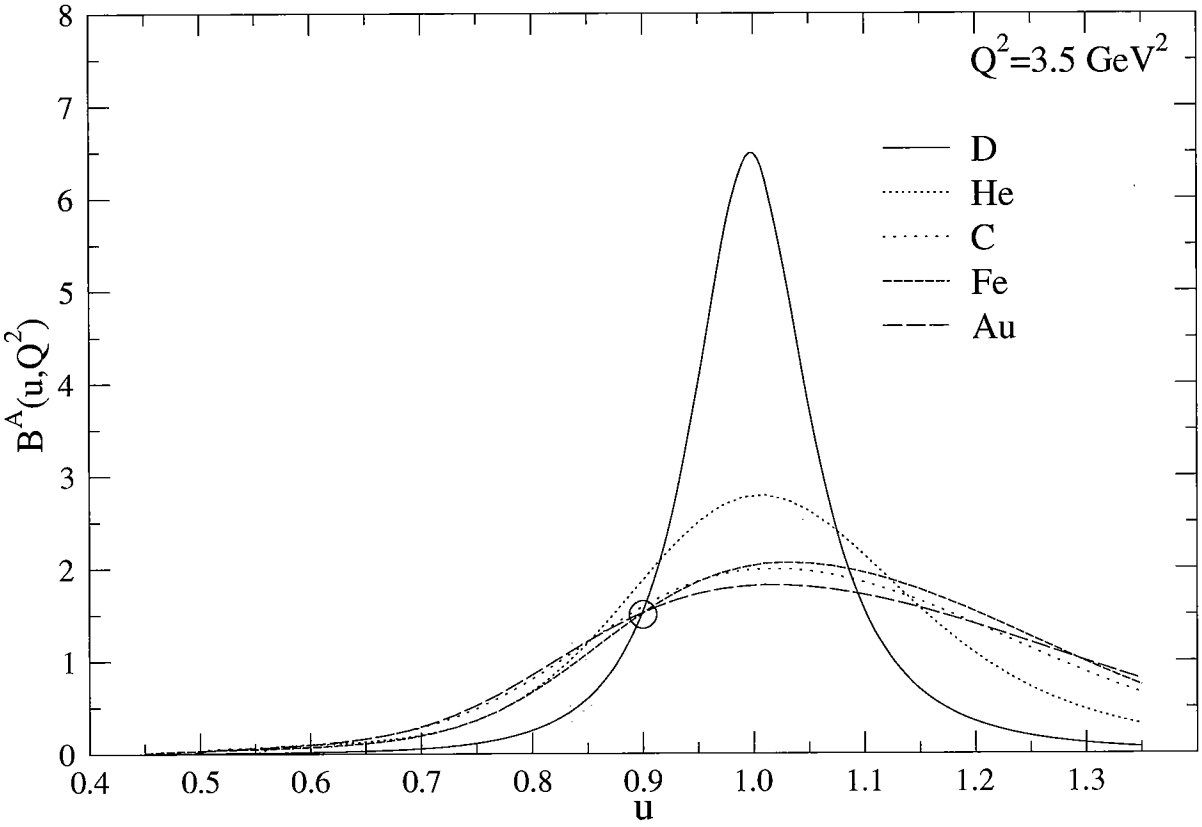

FIG. 4: The function $B^A(x, Q^2)$, Eq. (2.3) for our chosen targets at $Q^2 = 3.5\text{GeV}^2$. The circles mark the nearly identical crossing point u_i^A for D and $A > 4$, different from the same for ^{4}He and D.

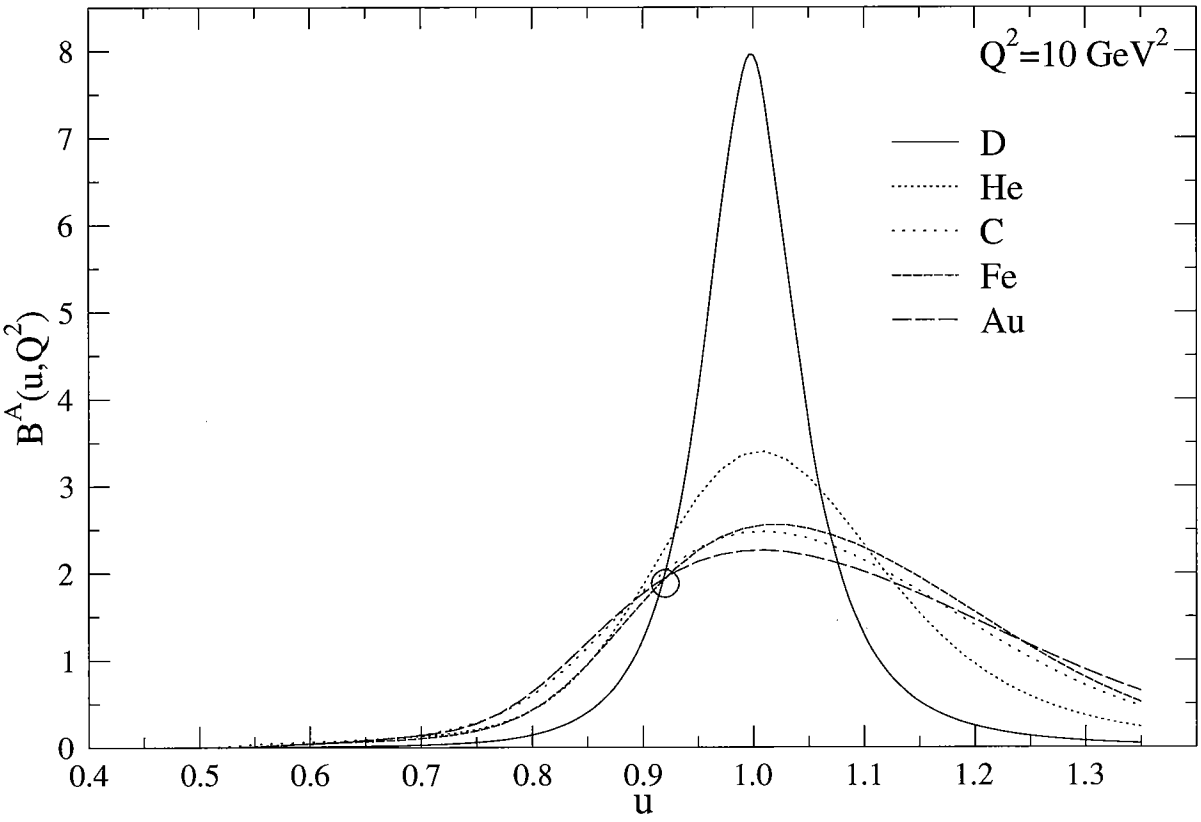

FIG. 5: Same as Fig. 4 for $Q^2 = 10$ GeV^2.

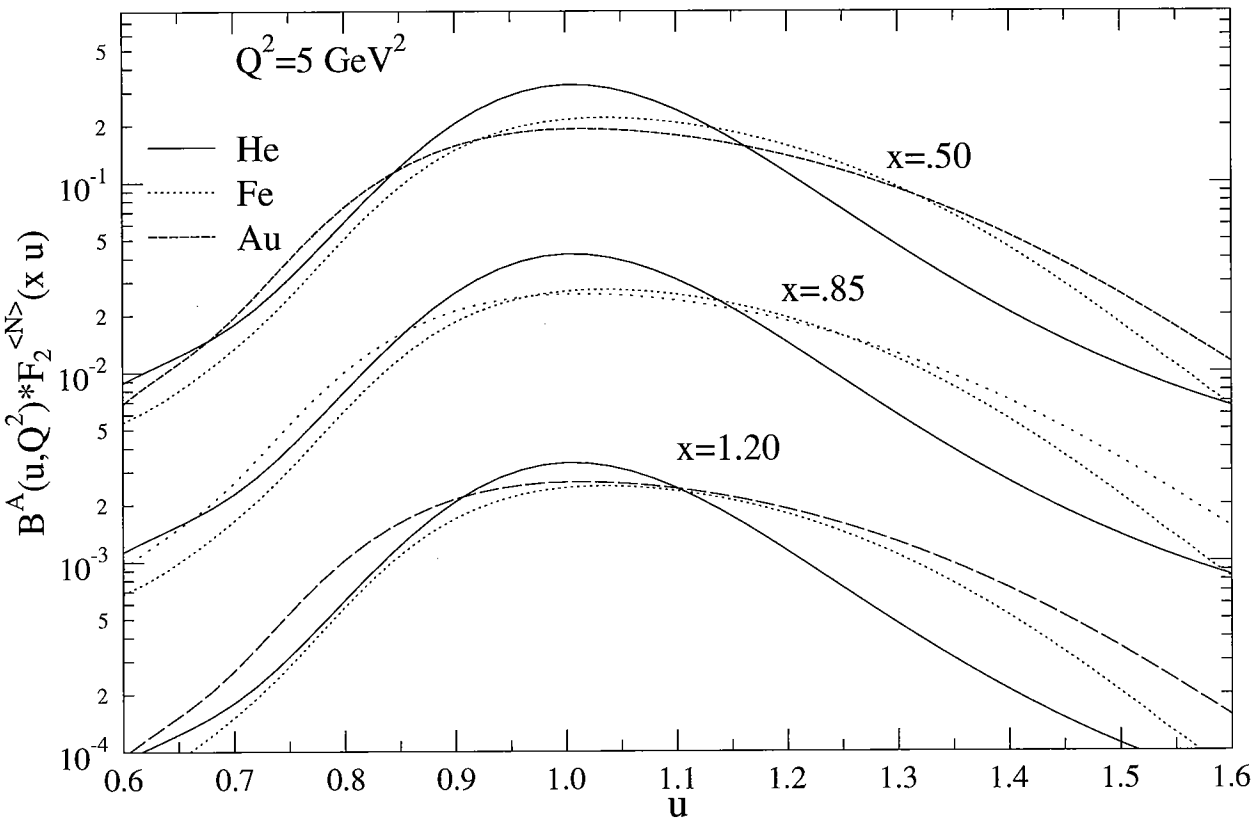

FIG. 6: The integrand $B^A(x,Q^2)F_2^{\langle N\rangle}(xu,Q^2)$ in Eq. (2.2), which determines the size of the integrals for F_2^A, for He, Fe, Au (drawn, dotted and dashed lines) and fixed $Q^2 = 5.0\,\mathrm{GeV}^2$. The sets of curves show, that the above products decrease about a factor of 10 for increasing $x = 0.5 \to 0.85 \to 1.2$.

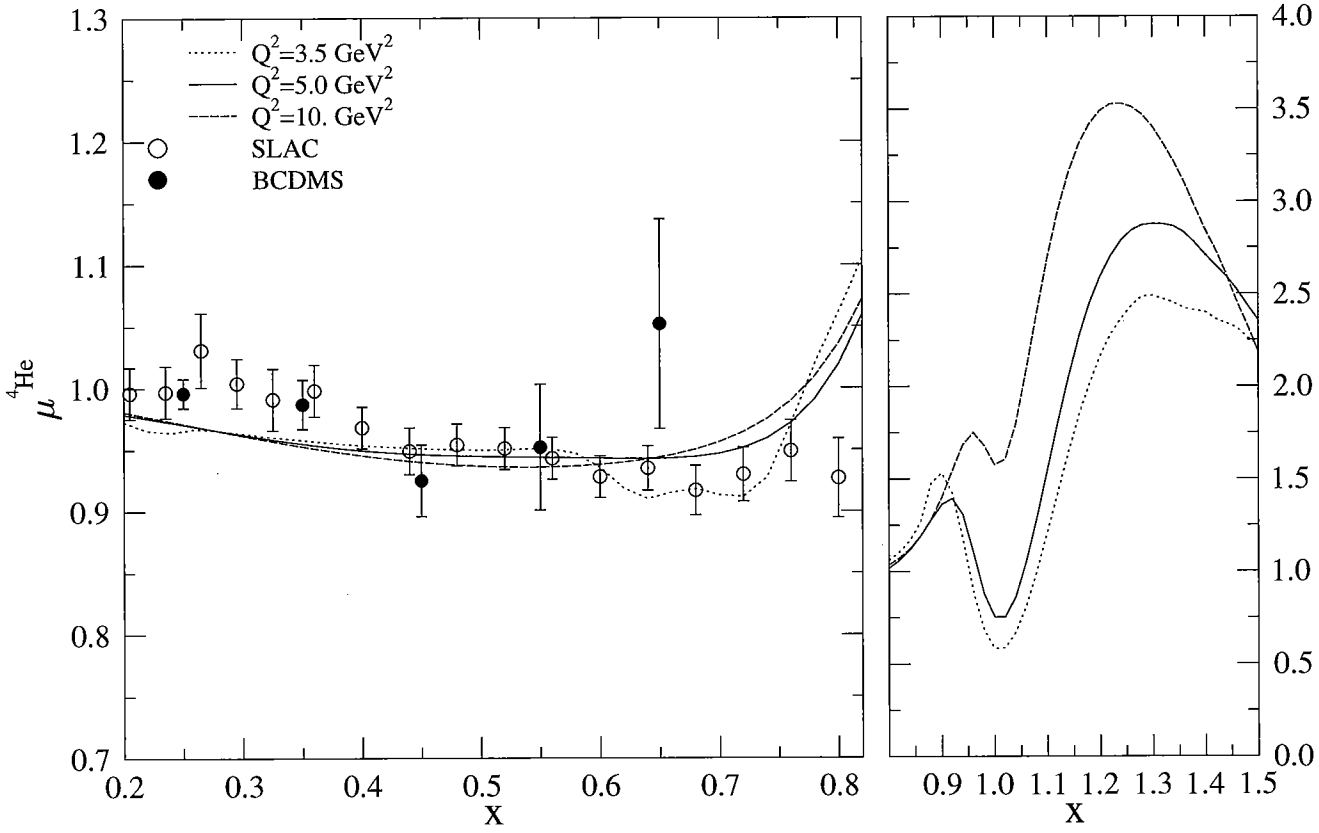

FIG. 7: $\mu^{^4\mathrm{He}}$ for $Q^2 = 3.5, 5.0, 10.0, \mathrm{GeV}^2$. Data in the classical range are from Ref. [42] (open circles) and Ref. [51] filled circles. No extracted data exist beyond that range.

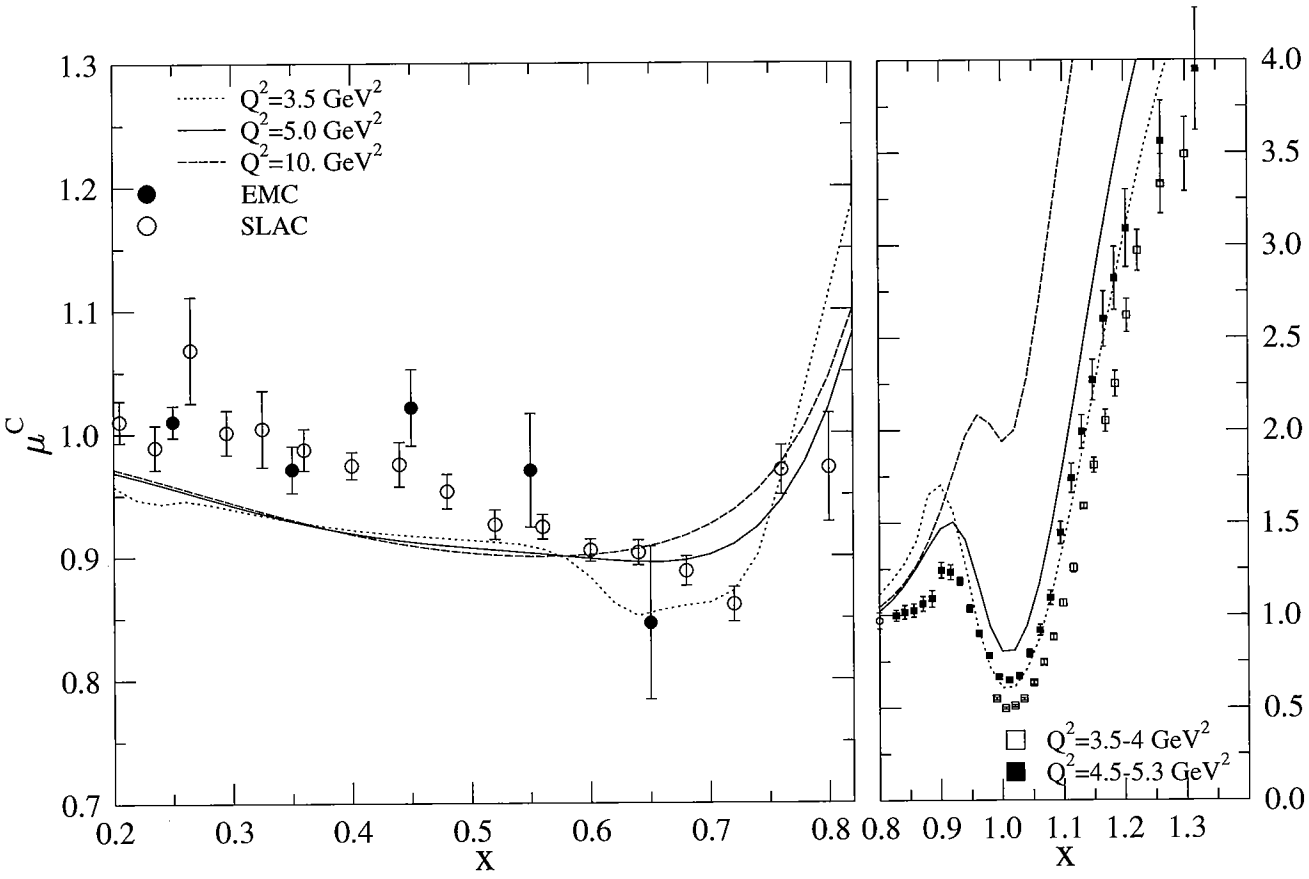

FIG. 8: Same as Fig. 7 for μ^C Data sets in the classical range are from Refs.[42, 52]. Extracted data are for varying $Q^2 \approx 3.5 - 4.2\,\mathrm{GeV}^2$ (open diamonds) and for varying $Q^2 \approx 4.5 - 5.2$ GeV^2 (filled diamonds) [14, 15]. Data are too sparse for interpolation towards $Q^2 = 3.5$ and $5.0\,\mathrm{GeV}^2$ for which calculated results are presented.

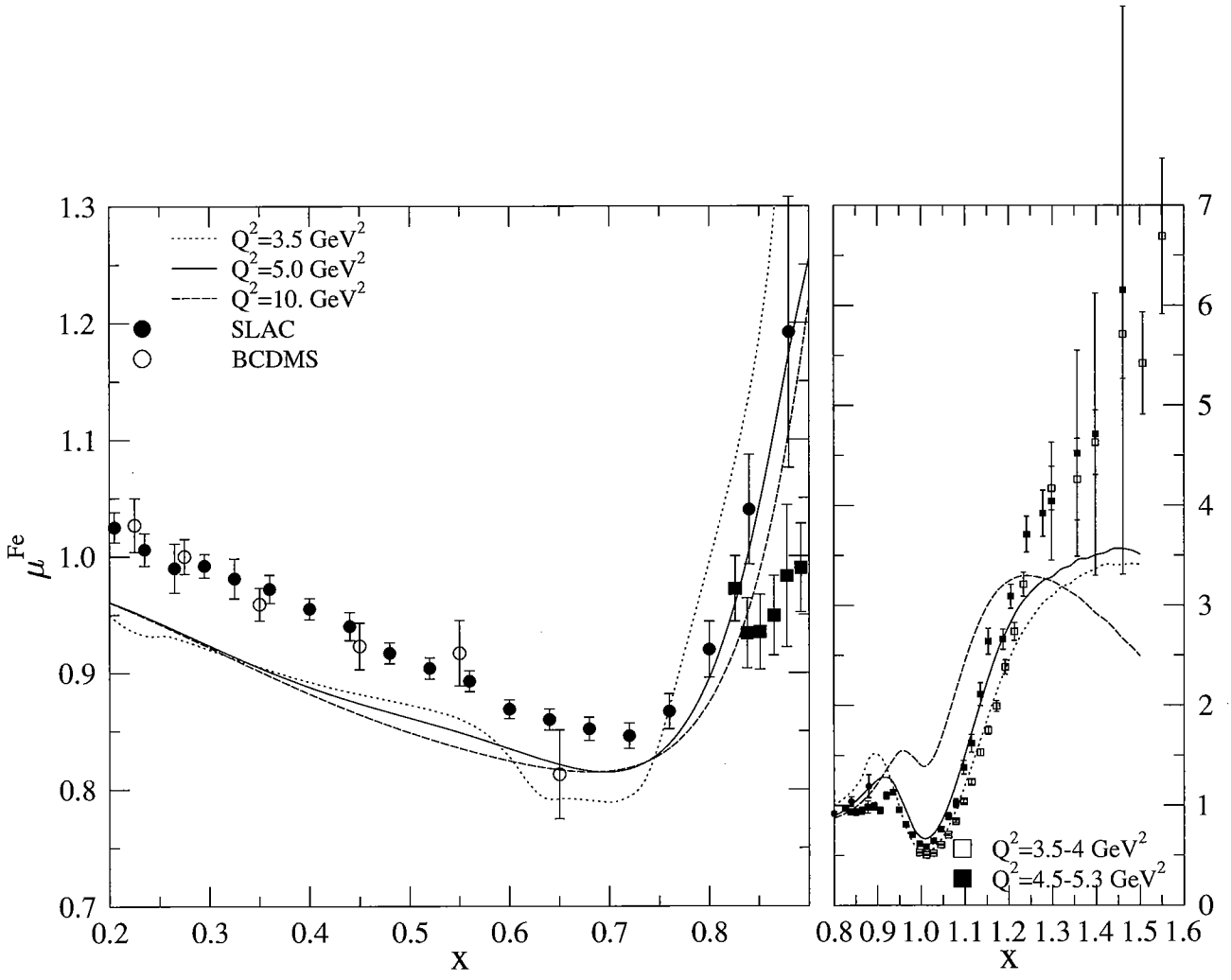

FIG. 9: Same as Fig. 7 for μ^{Fe} (Data from Refs. [42, 53]; see text in Section IV).

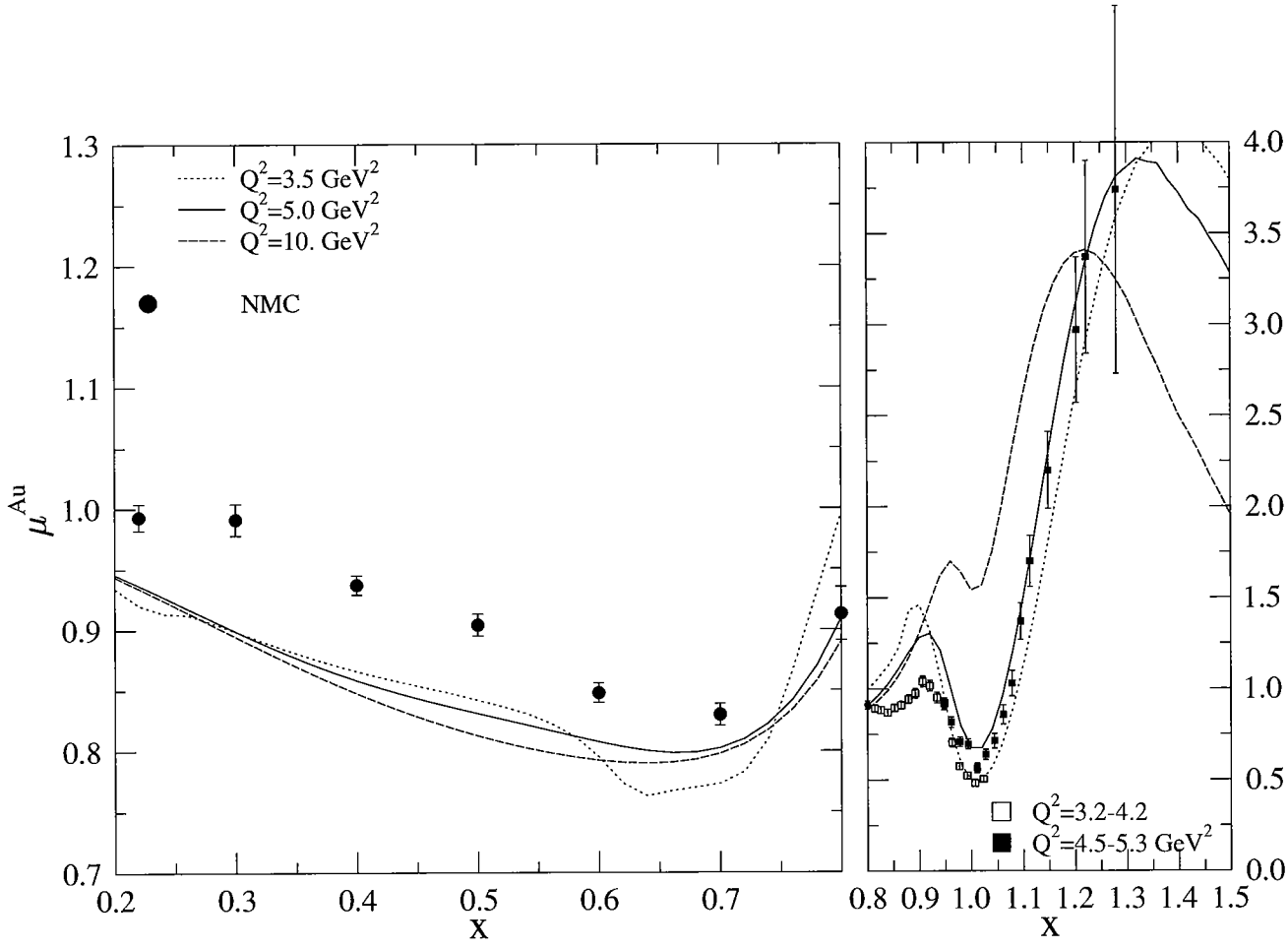

FIG. 10: Same as Fig. 7 for μ^{Au} (Data from Ref. [42]; see text in Section IV).

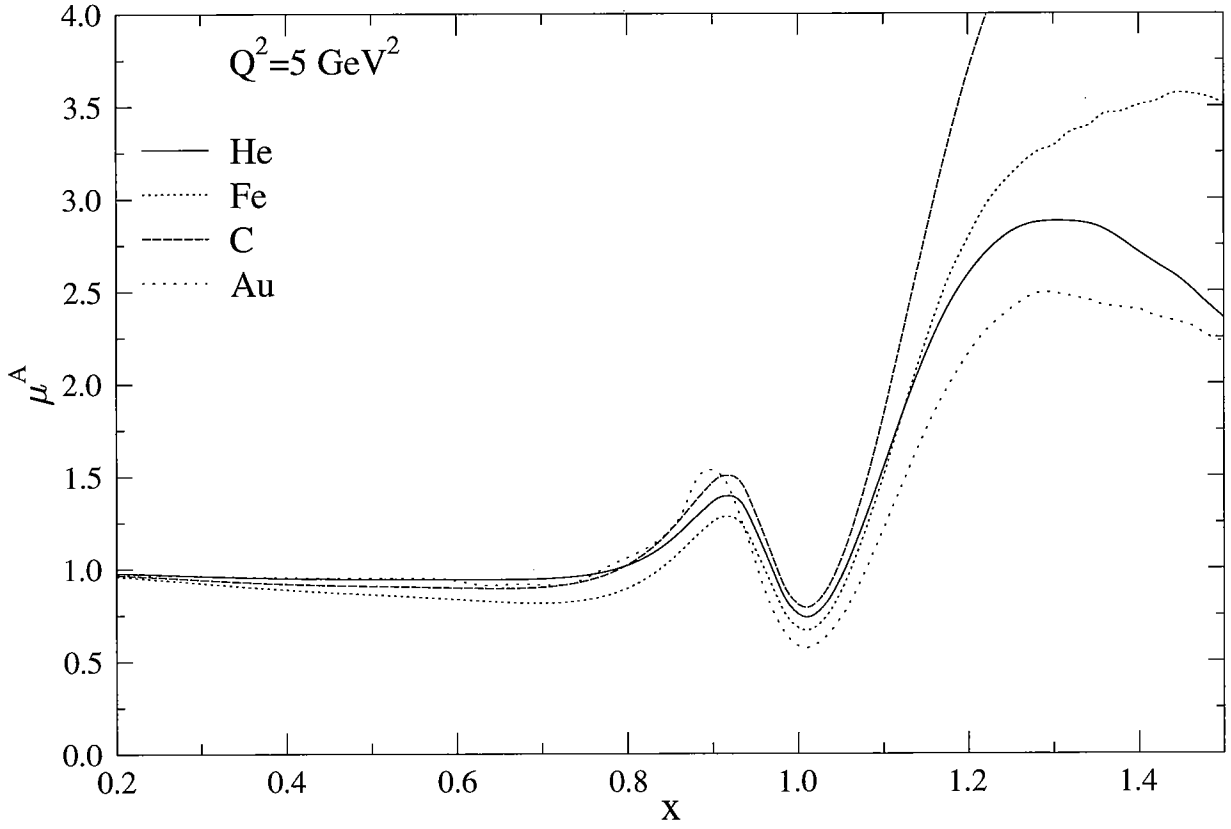

FIG. 11: A-dependence of computed EMC ratios.